

# THE STATUS OF THE IN-VACUUM APPLE II UNDULATOR IVUE32 AT HZB / BESSY II\*

J. Bahr<sup>†</sup>, J. Bakos, S. Gaebel, S. Gottschlich, S. Grimmer, C. Kuhn, S. Knaack, F. Laube, A. Meseck, C. Rethfeldt, E. Rial, A. Rogosch-Opolka, M. Scheer, P. Volz  
 Helmholtz-Zentrum Berlin, 12489 Berlin, Germany

## Abstract

At BESSY II, two new beamlines for RIXS and for X-Ray-microscopy need a short period variably polarizing undulator. For this purpose, the first in-vacuum APPLE II undulator worldwide is under construction. The parameters are as follows: *period length*  $\lambda_0 = 32\text{mm}$ , *# periods* = 78, *minimum gap* = 7mm. The design incorporates a force compensation scheme as proposed by two of the authors at the SRI 2018. All precision parts of the drive chain are located in air. New transverse slides for the transversal slit adjustment have been developed and tested. Optical micrometers measure the gap and shift positions, similar to the system of the CPMU17 at BESSY II. They provide the signals for motor feedback loops. A new UHV-compatible soldering technique, as developed with industry, relaxes fabrication tolerances of magnets and magnet holders and simplifies the magnet assembly. A 10-period prototype has been setup for lifetime tests of the new magnetic keeper design. The paper summarizes the status of the undulator IVUE32.

## INTRODUCTION

Photon beams with variably polarized light were already produced and used by the users in the 1980s at BESSY, the predecessor of BESSY II. BESSY II is a dedicated machine for soft X-ray photon production of arbitrary polarization with specific undulators. The low electron-beam energy of 1.7 GeV limits the fundamental photon energy range, and requires the usage of higher harmonics, e.g.: the 3<sup>rd</sup> harmonic for the transition metals and the 5<sup>th</sup> harmonic for the rare earth M-edges. Shorter periods lower the harmonic number and thus, enhance the brightness and the degree of polarization. Therefore, HZB launched the development of an in-vacuum APPLE II several years ago and published the design considerations and the mechanic layout at the IPAC 2018 [1].

The IVUE32 will serve two beamlines: A RIXS-beamline will use vertical linearly polarized photons in the range of 250-1000 eV for an efficient suppression of angle dependent optical effects. An X-ray microscope will operate in the range of 250-2500 eV, utilizing all polarization modes and the undulator harmonics 1–7.

In this paper, we focus on the new parts of the device and refer to [1] for the general design and the strategies, which did not change significantly. Meanwhile, the cast iron pieces and all components for the gap and phase motion are already fabricated. The bellows dimensions permit an

inclined mode operation, which requires a longitudinal range of  $\pm 16\text{mm}$ . Besides the inclined operation, the larger phase range (in the elliptical mode only  $\pm 8\text{mm}$  are required) bears more flexibility in the design of the RF-shielding system.

## TRANSVERSE SLIDES

After the IPAC 2018, we added transverse slides for the horizontal adjustment of the in-vacuum sub-girders. The slides employ two functions: i) the correction of geometric fabrication errors, ii) the correction of systematic field errors, where both errors may stay in relation, respectively. The slide adjustment provides an accuracy of  $20\mu\text{m}$  over a range of a few 0.1mm. The slides consist of two halves, which are preloaded with spherical washers. Adjustment plates with a specific thickness define the final position. A Dicronite-coating (<http://www.dicronite.de/>) guarantees a smooth sliding.

Only recently, we did a thorough analysis of systematic field errors and related phase errors of the IVUE32, and derived the tolerances of the in-vacuum girder bending. The analysis proved the viability of the slides for a precise horizontal slit adjustment [2].

In many cases, an analytic derivation of the phase error from a systematic field error is simple [2-4]. Usually, the probability distribution  $P(\Phi)$  of a systematic phase error is non-Gaussian. In many cases an analytic evaluation of this distribution for a strictly monotonic function is possible [5]. As an example, we illustrate the procedure for a linear taper, where  $s$  is the longitudinal coordinate and  $\Phi^{-1}$  the inverse function of  $\Phi$ :

$$\Phi(s) = s^2 \quad s = \Phi^{-1}(\Phi) = \sqrt{\Phi}$$

$$P(\Phi) = \partial(\Phi^{-1}(\Phi))/\partial\Phi = 1/(2\sqrt{\Phi})$$

If the phase function  $\Phi(s)$  is not strictly monotonic, it can be split in piece-wise strictly monotonic segments  $\Phi_i(s)$ , which can be treated with the procedure above, and a weighted sum of the contributions  $P_i(\Phi_i)$  yield  $P(\Phi)$ . Figure 1 gives a few examples for  $\Phi(s)$  and the related probability function  $P(\Phi)$ .

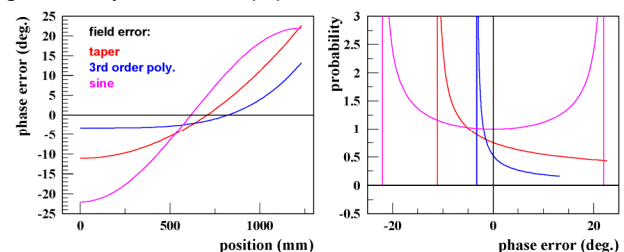


Figure 1: Examples of various systematic phase errors and their probability distributions as discussed in [2].

\* Work supported by ATHENA, a project of the Helmholtz Association.  
<sup>†</sup> johannes.bahr<sup>†</sup>@helmholtz-berlin.de

The rms-values of these phase distributions were derived analytically for several error types in [2-4]. An offset is subtracted from the phase distributions. The probability distributions are scaled vertically for better visibility.

### RF-SHIELDING SYSTEM

Different from the first ideas of a split liner as described in [1], the shielding of the magnet structure follows closely the strategy in planar IVUs and CPMUs, where a 100 μm CuNi foil is adopted. In this case the foil must be split longitudinally in order to permit the phase motion of the magnets. The foils are canted at the undulator center, and the short part is hidden in the slit between the magnet rows. Wakefields of geometric errors of the foil are expected to be low. Detailed simulation will start soon. The complete RF-shielding system is divided into four independent groups as depicted in Figure 2. A separation of the length adaption and the height adaption in to two independent units helps a lot. The RF-shielding system consists of the following groups:

- 8 foil tensioning systems
- bridging of small slits
- 8 height adaption units
- 8 length adaption units
- canted CuNi-foils on movable and fixed rows

The foil tensioning systems as well as the pieces for bridging small slits with CuNi-foil and RF-springs are adopted from the BESSY II CPMU17 [6]. The height adaption will be realized with a sliding, solid, indirectly cooled Cu-block, similar to the solution at NSRRC[7]. The other two components still need some development effort. The length adaption has to cover a range of  $\pm \lambda_0/2 = \pm 16mm$ . This is four times the range, which must be covered in the CPMU17 during cool-down. CPMUs in other laboratories demonstrated a safe handling of a much larger thermal shrinkage during cool-down even with an extended length and with Al-girders [7] instead of 1.4429 (CPMU), and thus, this issue is not regarded as a severe engineering challenge.

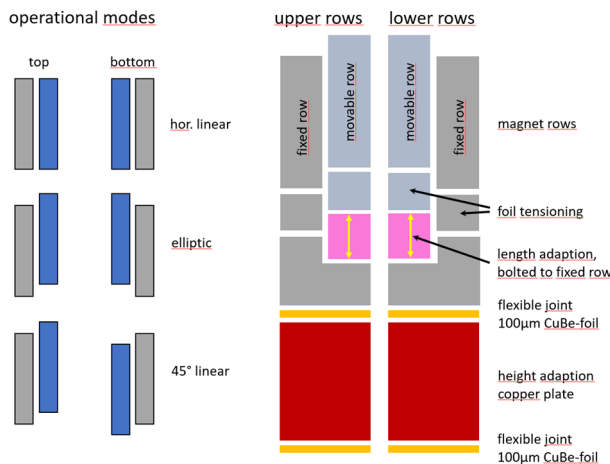


Figure 2: Independent components of the IVUE32 RF-shielding system.

The canted CuNi-foil needs some investigation in order to guarantee small geometric errors. The tolerances of these errors still have to be defined based on CST-simulations.

### UHV-COMPATIBILITY

The undulator must meet the UHV-requirements of the BESSY II machine. The chamber must be heated up to 200°C, whereas the magnets and specifically the magnet soldering must stay below 100°C. For this purpose an integrated water cooling of the four magnet subgirders was developed (Fig. 3). Each sub-girder employs two long holes. They are short-cut on one end, and at the other end two stainless steel water pipes are welded. The pipes go to the outside without further welding or brazing. The design guarantees a stressless operation of the water pipes inside the chamber during gap and phase motion. The bellows compensate for vertical and longitudinal motions. Figure 3, top shows the water cooling for two diagonal rows. The cooling of the opposite rows are connected to the opposite side of the chamber.

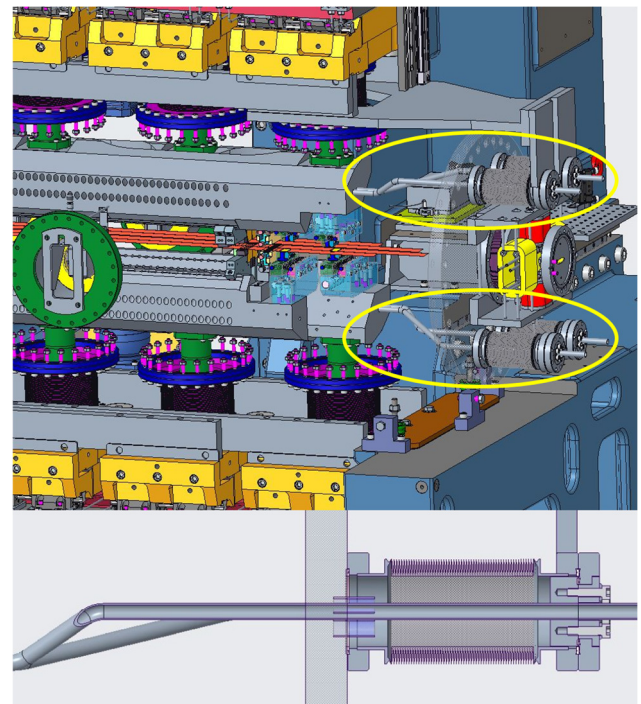


Figure 3: Water cooling of the four magnet sub-girders (yellow ellipses, top). A specific flange and a double-Cu-sealing (bottom) avoids critical couplings inside the UHV, which may leak.

### TESTING OF A TRANSVERSE SLIDE

An accurate horizontal alignment of the in-vacuum sub-girders will be done with five transverse slides per sub-girder. The procedure will be based on magnetic field measurements with an in-vacuum Hall-probe bench. The slides will be used for a phase shimming as well [2]. The transverse slides (Figure 3, top, yellow parts) define the parallelity of neighboring sub-girders. The slide stiffness is a critical number, which must be measured. The first slide

This is a preprint — the final version is published with IOP

Content from this work may be used under the terms of the CC BY 4.0 licence (© 2022). Any distribution of this work must maintain attribution to the author(s), title of the work, publisher, and DOI



Content from this work may be used under the terms of the CC BY 4.0 licence (© 2022). Any distribution of this work must maintain attribution to the author(s), title of the work, publisher, and DOI

has already been fabricated. Measurements with a specific measurement setup (Fig. 4) are on-going. We aim for the determination of the spring constant ( $\mu\text{m}/\text{kN}$ ) of the system slide/column, and the non-linearity. Both numbers will be compared to the FEM-results. After the successful test of the prototype, the other slides will be fabricated on a short time scale, since they are already pre-machined.

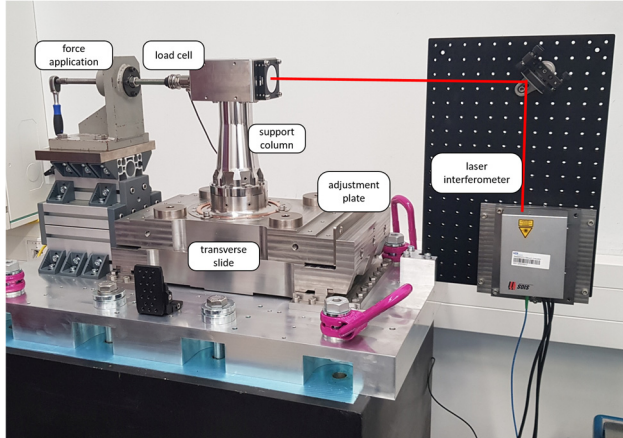


Figure 4: Test setup for the prototype transverse slide.

## 10-PERIOD PROTOTYPE AND ASSEMBLY OF FULL SCALE GIRDERS

One A- and one B-magnet (horizontal and vertical easy axis orientation) are soldered to a pair. This procedure replaces the magnet gluing of in-air APPLE II devices. The pair will be either soldered or clamped into the keeper. The soldering and clamping of the magnets will be checked carefully with a 10-period lifetime-test setup (Fig. 5), applying 850.000 full load cycles to the critical joints. The field integrals are measured regularly during the test. Loose connections will immediately be detected via the wire measurements.

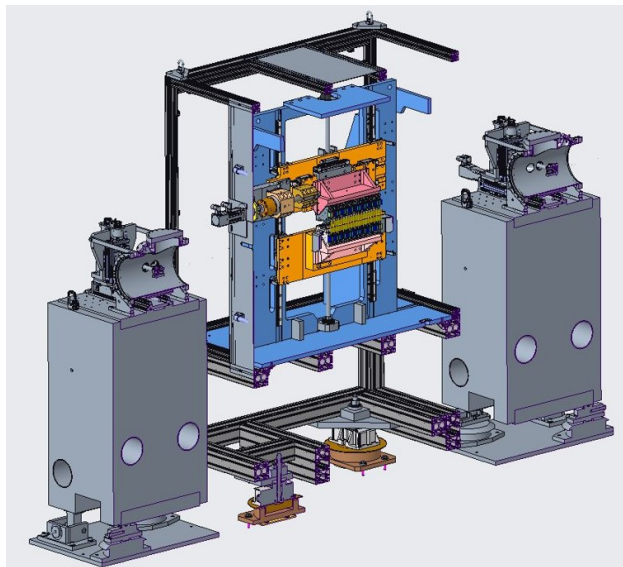


Figure 5: 10-period prototype. Half the structure is cut away for better visibility.

We established a strategy for a successive assembly of the four sub-girders. In the 1<sup>st</sup> step, the upper and the lower two sub-girders are assembled individually to pairs (Figure 6, top). The two sub-girders are shifted already by  $\lambda_0/4$  for minimum relative forces [8]. The assembly setup is located at a measurement bench, where the virtual shimming of complete keepers happens (functional magnets and compensation magnets installed). In the 2<sup>nd</sup> step, both sub-girder halves are combined in a similar procedure as for conventional in-air APPLE II (Fig. 6, bottom). In the 3<sup>rd</sup> step, the complete package rolls into the vacuum chamber, and each sub-girder is bolted individually to five columns after separation from the package.

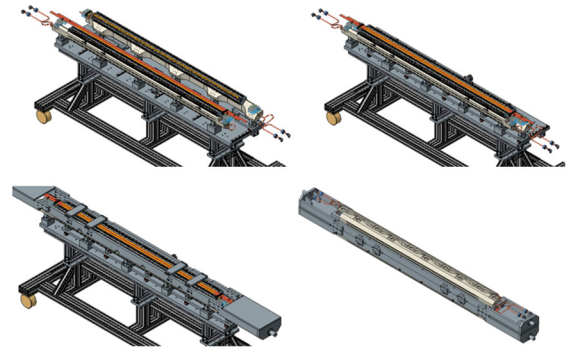


Figure 6: Successive assembly of the four sub-girders from top left to bottom right.

## REFERENCES

- [1] J. Bahrtd *et al.*, “In-Vacuum APPLE II Undulator”, in *Proc. IPAC’18*, Vancouver, Canada, Apr.-May 2018, pp. 4114-4116. doi:10.18429/JACoW-IPAC2018-THPMF031
- [2] J. Bahrtd *et al.*, “Phase Shimming of the in-Vacuum APPLE II at HZB / BESSY II with Transverse Slides”, *AIP Conf. Proc.*, SRI 2021, Hamburg Germany, vol. 1234, 2022, unpublished.
- [3] Y. Li, B. Faatz and J. Pflueger, “Undulator system tolerance analysis for the European x-ray free-electron laser”, *Phys. Rev. ST Accel. Beams*, vol. 11, p. 100701, 2008. doi:10.1103/PhysRevSTAB.11.100701
- [4] Y. Li, B. Ketengly and J. Pflueger, “Girder deformation related phase errors on the undulators for the European X-Ray Free Electron Laser”, *Phys. Rev. ST Accel. Beams*, vol. 18, p. 060704, 2015. doi:10.1103/PhysRevSTAB.18.060704
- [5] M. Titze, “Space Charge Modeling at the Integer Resonance for the CERN PS and SPS”, Doctoral Thesis at Humboldt University Berlin, 2019.
- [6] J. Bahrtd *et al.*, “Characterization and Implementation of the Cryogenic Permanent Magnet Undulator CPMU17 at Bessy II”, in *Proc. IPAC’19*, Melbourne, Australia, May 2019, pp. 1415-1418. doi:10.18429/JACoW-IPAC2019-TUPGW014
- [7] J.-C. Huang *et al.*, “Challenges of in-vacuum and cryogenic permanent magnet undulator technologies”, *Phys. Rev. ST - Accel. Beams*, vol. 20, p. 064801, 2017. doi:10.1103/PhysRevAccelBeams.20.064801
- [8] J. Bahrtd and S. Grimmer, “In-vacuum APPLE II undulator with force compensation”, *AIP Conference Proceedings*, vol.2054, p. 030031, 2019. doi:10.1063/1.5084594